

DOI: 10.19884/j.1672-5220.202303007

# Aurum-Mesh Transfer of Large-Scale Monolayer Graphene Patterns

LI Chao\*, JIANG Meng

College of Science, Donghua University, Shanghai 201620, China

**Abstract:** When graphene prepared by chemical vapor deposition (CVD) method is applied to various high-performance devices, graphene's transfer and patterning process usually reduces its intrinsic properties. A new method combining wet transfer and mechanical exfoliation can be utilized to accomplish high-quality and large-scale transfer of graphene patterns. This method requires the preparation of an aurum (Au)-mesh with pores of a specific form as the peeling belt. The contact area between the Au and graphene can offer sufficient adhesion to the homogeneous monolayer graphene for mechanical exfoliation, whereas the non-contact area between the hole and graphene has a relatively weak force to release the graphene patterns on the substrate. The surface morphology and electrical characterization of graphene show that the graphene surface is clean and uniform, while graphene field-effect transistors have high carrier mobility and small Dirac voltage. The Au-mesh transfer method can effectively improve the quality of the graphene patterns as well as the efficiency of the transfer, which opens up a broader scope for the application of CVD graphene and also provides a reference for the transfer of other CVD two-dimensional (2D) materials.

**Key words:** graphene transfer; graphene pattern; Au-mesh; lithography; transistor

**CLC number:** TN304.9

**Document code:** A

**Article ID:** 1672-5220(2024)03-0241-08

Open Science Identity  
(OSID)



## 0 Introduction

Microelectronic technology is evolving along Moore's law and is approaching its physical limits. The outstanding electrical properties of graphene make it the most competitive channel material to replace silicon (Si) in the post-Si complementary metal oxide semiconductor era. Optimization and maturation of the graphene preparation process is a prerequisite for subsequent applications. Chemical vapor deposition (CVD) method, epitaxial growth method<sup>[1]</sup> and oxide reduction method<sup>[2]</sup> are the common methods used to synthesize graphene. Among them, CVD is scalable to generate high-quality graphene. Graphene has been synthesized on various metal

substrates including copper<sup>[3-4]</sup>, ferrum<sup>[5]</sup>, ruthenium<sup>[6]</sup>, cobalt<sup>[7]</sup>, iridium<sup>[8]</sup>, nickel<sup>[9]</sup>, platinum<sup>[10]</sup>, aurum (Au)<sup>[11]</sup> and germanium (Ge)<sup>[12-13]</sup>. Preparation of high-quality graphene cannot avoid the use of metal substrates. Subsequent applications must transfer graphene from the metal substrate to the desired insulating or semiconductor substrate<sup>[14]</sup>. However, the transfer process is prone to material contamination and damage, which affects the large-scale promotion and application. Therefore, there is an urgent need to develop advanced transfer techniques to promote the application of CVD graphene. The advancement of transfer methods plays an important role in the study and application of graphene films<sup>[15-16]</sup>. The non-toxic, environment-friendly and easy-to-process properties of polymethyl methacrylate (PMMA) make it a perfect material for promoting graphene transfer. However, the covalent interaction between the defects on the graphene surface and the PMMA layer makes it difficult to remove PMMA. Even after thorough washing with organic solvents, such as trichloromethane (TCM) or acetone, a tiny coating of residual molecules can adhere to graphene<sup>[17-18]</sup>. Graphene transferred using the PMMA method is heavily contaminated, which also reduces its electrical properties.

In this paper, we report a combined method for transferring monolayer graphene grown on Ge(110), and the process involves wet transfer followed by mechanical exfoliation using an Au-mesh tape<sup>[12-13]</sup>. Compared to the typical mechanical exfoliation method, i. e., scotch tape strips off the bulk materials<sup>[19]</sup>, one advantage of the Au-mesh transfer method is that it improves the size and the yield of the two-dimensional (2D) materials. During Au-mesh transfer, the contact area between Au and graphene can offer sufficient adhesion to allow graphene to be exfoliated uniformly, whereas the non-contact area provides a weak interaction to mechanically release graphene on the target substrate. In the Au-mesh transfer method, the polycarbonate (PC) film serving as a support layer is easily removed<sup>[20]</sup> and the Au-mesh serving as a mask for patterning processes<sup>[21]</sup> is peeling off during mechanical exfoliation without etching. The graphene patterns are the graphene at the holes of the Au-mesh, thus avoiding the defects and strains introduced

Received date: 2023-03-14

\* Correspondence should be addressed to LI Chao, email: 2202247@mail.dhu.edu.cn

Citation: LI C, JIANG M. Aurum-mesh transfer of large-scale monolayer graphene patterns [J]. *Journal of Donghua University (English Edition)*, 2024, 41(3): 241-248.

during the deposition of the metal. The process does not use organic polymer layers or iodine compounds for etching, thus allowing high-quality 2D monolayer patterning for large-scale exfoliation. In the traditional patterning process, plasma penetrates the edge of the photoresist during the reaction ion etching (RIE) process, and the graphene underneath the photoresist is partially knocked off, making the target pattern irregular and unclear at the edges. Another advantage of the Au-mesh transfer method is that the patterning process does not require RIE, thus avoiding the problem of graphene patterns being destroyed by plasma. Additionally, we fabricate a single-layer graphene field-effect transistor (GFET) with a field-effect carrier mobility of approximately  $500 \text{ cm}^2/(\text{V} \cdot \text{s})$  and a drive current of  $121 \text{ A/m}$  by the Au-mesh transfer method without an additional etching process. We speculate that this work will be combined with the work on van der Waals integration<sup>[22-24]</sup> to obtain a high-quality metal-semiconductor interface. This work would provide a simple and scalable method for stripping patterns of 2D materials, and facilitate fundamental research on materials and practical device applications.

## 1 Experimental Section

### 1.1 Growth and characterization of graphene/Ge(110)

The CVD method is used to prepare monolayer graphene on Ge(110) substrates. The CVD method involves decomposing hydrocarbon precursor ( $\text{CH}_4$ ) at high temperatures and depositing the decomposition products on a metal substrate to generate monolayer or multilayer graphene. The Ge(110) surface covered by a single layer of graphene cannot continue to catalyze the decomposition of  $\text{CH}_4$ , and thus the graphene growth process is terminated. Due to this self-limiting effect, graphene grown on Ge(110) remains strictly as a monolayer.

The Ge(110) substrate, sapphire sheet and quartz tray are cleaned, and the polished side of the Ge(110) substrate is inverted onto the rough surface of the sapphire

sheet to avoid contamination caused by impurity particles deposited onto the surface of the Ge(110) sheet during the growth process. As shown in Fig. 1(a), the sapphire sheet is placed in the center of the quartz tray and pushes the quartz tray to the center of the heating zone. The vacuum valve is opened and the tube is evacuated to below 10 Pa. The tube is flushed with Ar at a flow rate of  $800 \text{ cm}^3/\text{min}$  for 5 min. Then, the vacuum valve is closed, and the growth parameters are input into the computer control software. The growth procedures of graphene are divided into heating stage, growth stage and cooling stage, as shown in Fig. 1(a). In the heating stage, the gas mixture of Ar and  $\text{H}_2$  with a volume ratio of 10 : 1 is flowed through the tube. The heating stage is set to heat up to  $916 \text{ }^\circ\text{C}$  in 120 min. In the growth stage, the gas mixture of  $\text{CH}_4$ , Ar and  $\text{H}_2$  with a volume ratio of 1 : 350 : 35 is flowed through the tube. The growth stage is set to hold at  $916 \text{ }^\circ\text{C}$  for 480 min. In the first cooling stage, the gas mixture of Ar and  $\text{H}_2$  with a volume ratio of 15 : 1 is flowed through the tube. The first cooling stage is set to reduce the temperature to  $400 \text{ }^\circ\text{C}$  in 60 min. In the second cooling stage, the gas mixture of Ar and  $\text{H}_2$  with a volume ratio of 20 : 1 is flowed through the tube. The second cooling stage is set to reduce the temperature to  $100 \text{ }^\circ\text{C}$  in 60 min. Raman spectroscopy is performed on the graphene samples. The Raman spectrum for graphene is shown in Fig. 1(b), and the value of the peak 2D/G of graphene Raman signal is higher than 2, which means that the graphene is monolayer graphene. There is no signal of defective D peaks in the Raman spectrum, indicating the graphene is of high quality with few defects. This section solely provides an explanation of the Raman spectroscopy of graphene from the perspective of the experimental method, aiming to initially demonstrate the feasibility of the experimental approach. Detailed interpretations of the D peak, G peak and 2D peak in the Raman spectra, as well as the fitting and peak intensity calculations, will be addressed in Section 2. Figure 1(c) shows a height map of the atomic force microscopy (AFM) test, in which the graphene folds and atomic steps of the Ge(110) substrate are clearly visible.

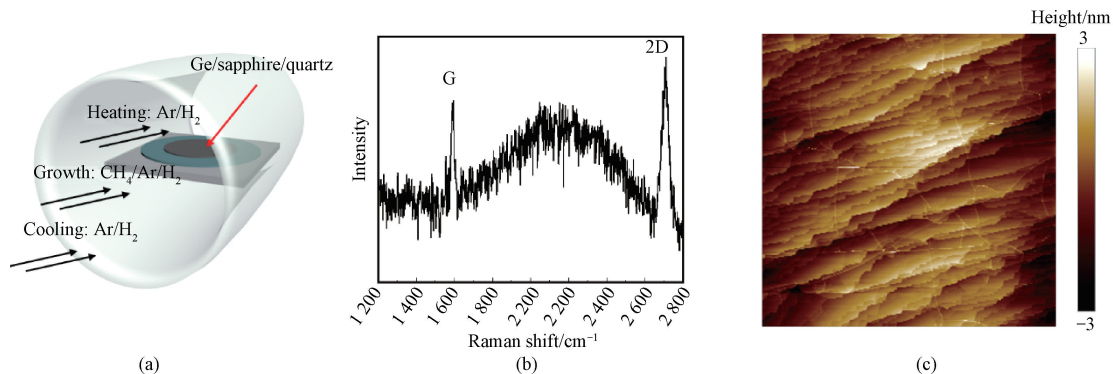


Fig. 1 Characterization of graphene/Ge(110): (a) CVD system; (b) Raman spectrum; (c) AFM height map

### 1.2 Transfer of graphene patterns

By creating an Au-mesh with pores of a certain form as the peeling belt, we present a novel approach that combines wet transfer and mechanical exfoliation to facilitate the preparation of high-quality and large-scale graphene. Figure 2 shows the schematic diagram of the Au-mesh for mechanical exfoliation. As shown in

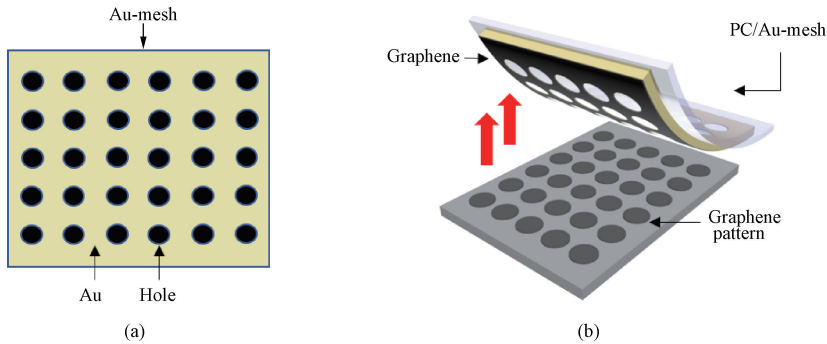


Fig. 2 Schematic diagram of Au-mesh for mechanical exfoliation: (a) Au-mesh with specific shape array; (b) transfer of graphene patterns

Figure 3 shows the schematic illustration of the Au-mesh transfer process, which combines wet transfer and mechanical exfoliation. A mesh structure is first defined via UV lithography and developing techniques on a Ge(110) based monolayer graphene. A 50 nm thick gold film is deposited on the graphene/Ge(110) with the defined mesh structure. After completion of the metal lift-off process, a PC polymer layer is spin-coated (4 000 r/min, 60 s) onto the sample as a support layer to assist in the detachment of the Au-mesh and graphene from Ge(110). The samples are then floated in an HF/H<sub>2</sub>O<sub>2</sub> solution for 5 h to etch away the Ge(110) substrate. After that, the samples are placed onto SiO<sub>2</sub>/Si substrates after rinsing thrice with deionized water. As far as possible, we avoid wrinkles and bubbles in the transfer process through natural drying and micro-heating treatment, so that the PC/Au-mesh/graphene and SiO<sub>2</sub>/Si sheet become more

fitting. This method improves the success of wet transfer. Tweezers or polyimide (PI) strips can tear PC and the Au-mesh directly from SiO<sub>2</sub>/Si after heating (130 °C for 5 min). Thus, the tape easily exfoliates the continuous and uniform monolayer graphene pattern arrays. TCM could quickly and effectively remove the PC layer, which significantly lowers the residue. However, the graphene sheet would be damaged or torn during the rapid dissolution of the PC film in TCM<sup>[20]</sup>. The Au-mesh transfer method has the advantage that the processing time is short because of the low amount of PC residue. The destruction of graphene by TCM during the rapid removal of the PC is avoided. Treatment with TCM is helpful for obtaining higher-quality graphene in Au-mesh transfer because PC can be easily removed with TCM. However, the p-doping effect caused by TCM processing must be considered, which can be mitigated by the annealing process<sup>[25]</sup>.

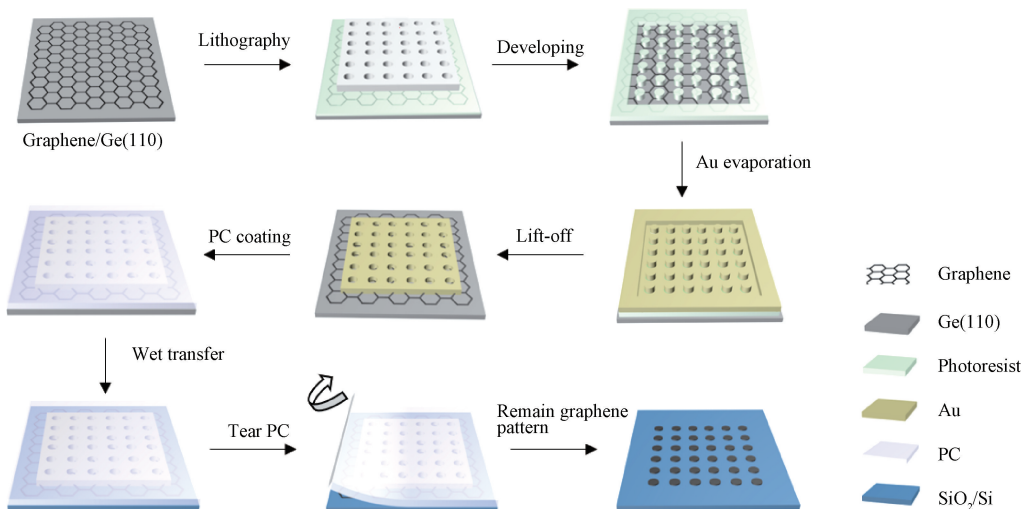


Fig. 3 Schematic illustration of Au-mesh transfer process

Meanwhile, because of the presence of the Au-mesh on PC, the PC support layer becomes stronger, making the wet transfer process easy to operate. The Au-mesh transfer method is free of RIE steps for fabricating 2D material patterns, and thus the experimental process is shorter and simpler. Moreover, this transfer technique is applicable not only to graphene but also to other 2D materials, which can improve the quality and the scalability of these 2D materials.

### 1.3 High-performance monolayer graphene transistor

With the ability to peel off graphene patterns on target substrates, we can construct an Au-mesh of channel-shaped holes to strip the channel graphene without an additional channel patterning process. Figure 4 shows a schematic of the GFET structure, with Au as the electrode,  $\text{Al}_2\text{O}_3$  as the gate medium, and graphene transferred by the Au-mesh as the channel. The source and the drain electrodes are first defined by UV lithography and electron beam evaporation deposition of metal materials (50 nm Au) on CVD graphene/Ge (110). A 3 nm thick Al layer is evaporated using an electron beam. Then, a gate dielectric of 30 nm  $\text{Al}_2\text{O}_3$  is deposited by atomic layer deposition (ALD). After deposition of the gate dielectric, the pattern of the gate dielectric is defined by UV lithography, and then the excess dielectric is etched off. The top gate (50 nm Au) is defined using the same method as the source electrode.

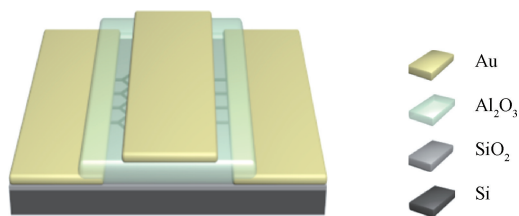


Fig. 4 Schematic of GFET

## 2 Results and Discussion

### 2.1 Characterization of graphene patterns

The method we demonstrate can be used to transfer monolayer graphene patterns onto a substrate. As shown in Fig. 5, different shapes of graphene patterns are transferred on  $\text{SiO}_2/\text{Si}$  sheet using the Au-mesh transfer method. Monolayer graphene patterns of triangle (Fig. 5(a)), circle (Fig. 5(b)) and square (Fig. 5(c)) are successfully generated on  $\text{SiO}_2/\text{Si}$  sheet by predesigning Au-meshes of different hole shapes. As shown in Fig. 5(c), the maximum size of the square pattern is  $20\ \mu\text{m} \times 20\ \mu\text{m}$ . The existence of a large non-contact area between graphene and the holes leads to a decrease in the spalling rate but an increase in graphene cracking. Effectively enhancing the exfoliation success rate can be achieved by improving the adhesion of the substrate through the application of a functional layer of polyvinyl alcohol (PVA)<sup>[21]</sup>.

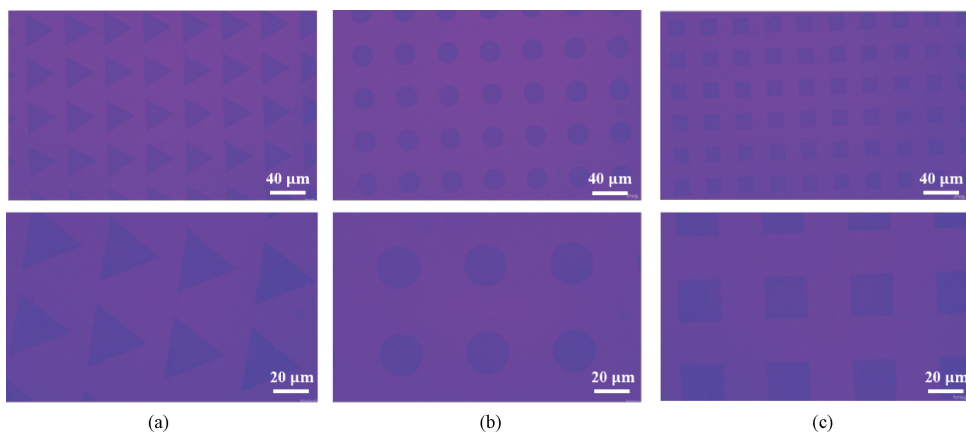


Fig. 5 Images of monolayer graphene patterns with different shapes: (a) triangle; (b) cycle; (c) square

Graphene patterns are left on  $\text{SiO}_2/\text{Si}$  sheet after tearing the Au-mesh with a PC. The D peak, G peak and 2D peak are characteristic peaks in the Raman spectrum of graphene, and their appearance and intensity provide important information about the structure and properties of graphene. The intensity of the D peak is related to the number of defects or impurities in graphene. The G peak represents the vibrational mode  $E_{2g}$  in graphene, and the 2D peak represents the two-photon process in the graphene lattice. The intensity ratio of the 2D peak to the G peak ( $I_{2D}/I_G$ ) is used to determine the number of

layers in a graphene sample and the effect of factors such as impurities on graphene. Typically,  $I_{2D}/I_G$  of monolayer graphene is around 2, while the ratio of multilayer graphene is smaller.  $I_{2D}/I_G$  can also be used to evaluate the quality and crystallinity of graphene. If the 2D peak is weak, then  $I_{2D}/I_G$  is smaller, indicating that impurities and defects have a greater effect on graphene.

The peak position,  $I_{2D}/I_G$  and the full width at half maximum (FWHM) of the 2D band can be used to estimate graphene quality<sup>[26]</sup>. The tiny D peak indicates that high-quality monolayer graphene is transferred from

the Au-mesh. We also perform the PMMA transfer process. The differences in the characterization of graphene obtained by the two transfer methods are not significant from the Raman spectra (Fig. 6(a)), which is expected since both methods are based on the same wet transfer process. The comparison graph shows that the graphene transferred by Au-mesh has a larger  $I_{2D}/I_G$  value. The inset is a partial enlargement of the Raman shift at  $1\,250\text{--}1\,450\text{ cm}^{-1}$ . From the inset, it can also be seen that the graphene transferred by the Au-mesh has smaller defective D peak. Both of these values indicate that the graphene transferred by the Au-mesh transfer method is of higher quality. As shown in Fig. 6, Raman spectral mapping is performed across a  $10\text{ }\mu\text{m}\times 10\text{ }\mu\text{m}$  region for analysis.  $I_{2D}/I_G$  is approximately 2.1

and the 2D FWHM is approximately  $35\text{ cm}^{-1}$ , which is the signal of high-quality monolayer graphene. The uniform intensity of the exfoliated graphene patterns is also confirmed using Raman mapping, as shown in Figs. 6(c) and 6(d). Subsequently, tapping mode measurements are conducted using AFM to verify the presence of residual contaminants on the graphene surface. Figure 6(b) shows an AFM image of a monolayer of graphene after transfer using Au-mesh with a root mean square (RMS) roughness of 0.8 nm. This indicates that very little residue remains during the transfer process. Accordingly, these results show that the Au-mesh layer effectively obtains a large area of clean graphene patterns.

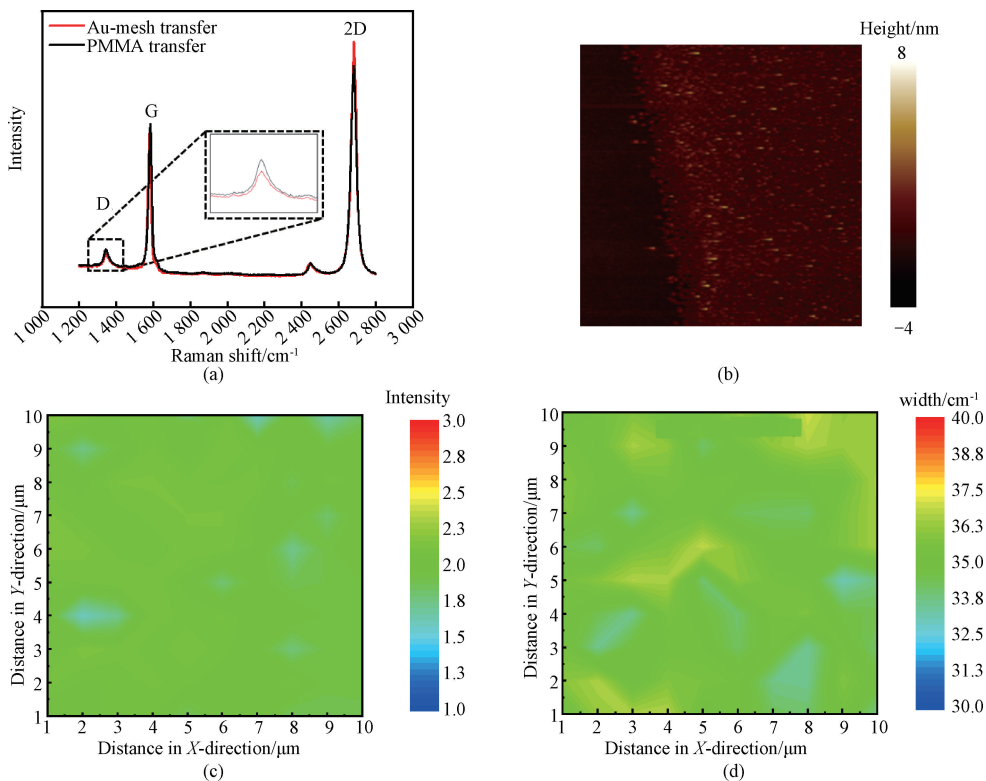


Fig. 6 Characterization of graphene patterns: (a) Raman spectra; (b) AFM; (c)  $I_{2D}/I_G$  of Raman intensity map; (d) Raman intensity map of 2D FWHM

## 2.2 Characterization of electrical properties

Figure 7(a) is a scanning electron microscope (SEM) image of GFET with a dual-finger gate and ground-signal-ground (GSG) structure. In Fig. 7(b), the lines represent the measured output characteristic curves of the GFET. The source-drain current  $I_{ds}$  shows a linear increase as the source-drain voltage  $V_{ds}$  increases (the maximum  $V_{ds}$  is 1.0 V). The  $I_{ds}$  values are

measured at a constant gate bias voltage  $V_{gs}$  of 0, 0.8, 1.6, 2.4, 3.2 and 4.0 V by sweeping  $V_{ds}$  from 0 to 1.0 V. By applying 0.1, 0.3, 0.5, 0.7, 0.9 and 1.0 V source-drain voltages respectively, a typical transfer curve is shown in Fig. 7(c), with significant p-type behavior. The GFET exhibits high electrical performance, mainly owing to the low residuals in the channel area.

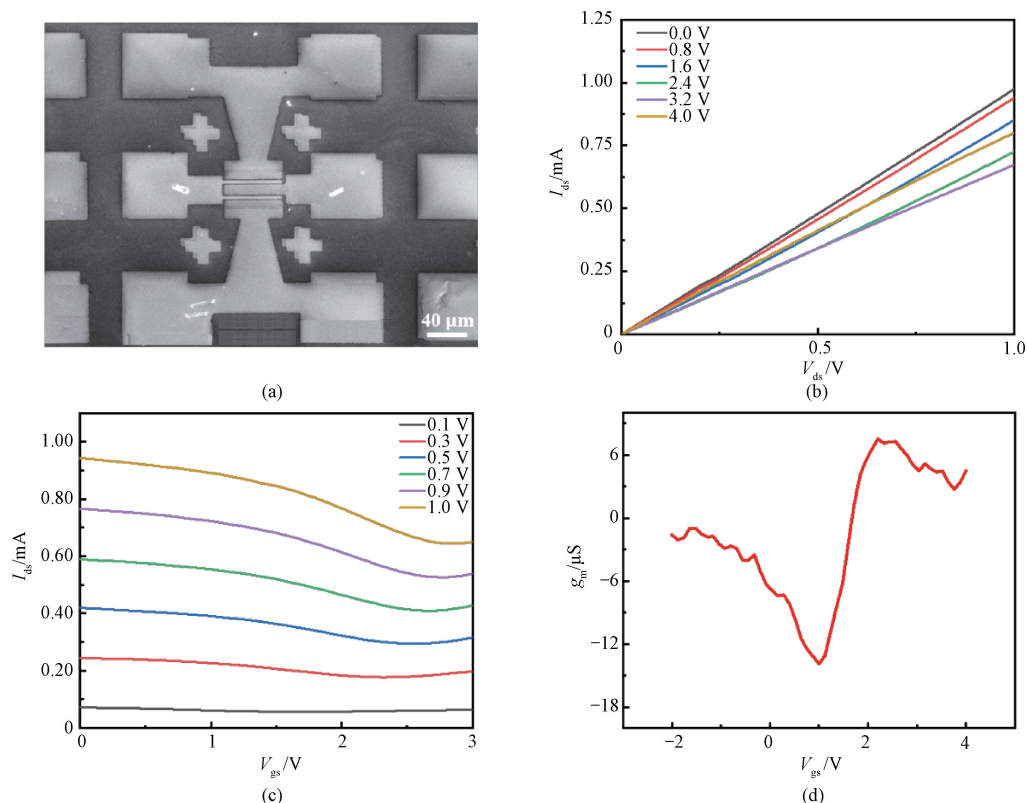


Fig. 7 Characterization of electrical properties of GFET; (a) SEM image of GFET on  $\text{SiO}_2/\text{Si}$  substrate; (b) output characteristic curves; (c) transfer curves; (d) transconductance curve

The carrier mobility of GFET  $\mu$  is calculated from the transconductance:

$$\mu = \frac{g_m}{C_{\text{ox}} V_{\text{ds}}} \frac{L}{W} \quad (1)$$

where  $g_m$  is the transconductance at a source-drain voltage of 0.1 V;  $C_{\text{ox}}$  is the capacitance value of per unit area;  $L/W$  is the ratio of the channel's length to its width ( $8 \mu\text{m}/20 \mu\text{m}$ ). The capacitance value obtained from the capacitance-voltage ( $C$ - $V$ ) test is divided by the effective capacitance area ( $5 \mu\text{m} \times 50 \mu\text{m}$ ) between the source (drain) and the top gate to obtain a  $C_{\text{ox}}$  value of  $0.11 \times 10^{-6} \text{ F/cm}^2$ . The field-effect carrier mobility of the device reaches  $500 \text{ cm}^2/(\text{V} \cdot \text{s})$ . The Au-mesh transfer yields the surface-clean graphene, which reduces the contact resistance between the electrode and graphene. This improves the electrical performance and increases the driving current. In other words, Au-mesh transfer is a viable alternative to PMMA transfer.

### 3 Conclusions

In summary, we report a new CVD graphene transfer method in which monolayer graphene patterns with various shapes can be achieved by means of a prefabricated Au-mesh while maintaining their quality. The transferred monolayer graphene patterns exhibit

excellent electrical properties. Moreover, the entire transfer process does not require additional etching to obtain the exact shape of the patterns. The intrinsic characteristics of the exfoliated monolayer graphene are confirmed using a variety of characterization techniques. This research has the potential to increase the use of CVD graphene in areas where clean graphene transfer conditions are required. This method of transferring large-scale graphene patterns will promote the wide application of CVD graphene in electronic devices.

### References

- [ 1 ] LU H, LIU W J, WANG H L, et al. Molecular beam epitaxy growth and scanning tunneling microscopy study of 2D layered materials on epitaxial graphene/silicon carbide [ J ]. *Nanotechnology*, 2023, 34(13): 132001.
- [ 2 ] XING W Q, HU J M, ZHANG X. Electrochemical reduction determination of *N*-nitrosodiphenylamine in food based on graphene electrode material [ J ]. *Journal of Donghua University (English Edition)*, 2022, 39(2): 128-133.
- [ 3 ] LI X S, CAI W W, AN J, et al. Large-area synthesis of high-quality and uniform graphene films on copper foils [ J ]. *Science*, 2009, 324(5932): 1312-1314.

- [ 4 ] LEE Y, BAE S K, JANG H, et al. Wafer-scale synthesis and transfer of graphene films [ J ]. *Nano Letters*, 2010, 10(2) : 490-493.
- [ 5 ] AN H, LEE W J, JUNG J. Graphene synthesis on Fe foil using thermal CVD [ J ]. *Current Applied Physics*, 2011, 11(4) : S81-S85.
- [ 6 ] SUTTER E, ALBRECHT P, SUTTER P. Graphene growth on polycrystalline Ru thin films [ J ]. *Applied Physics Letters*, 2009, 95(13) : 113109.
- [ 7 ] WANG S M, PEI Y H, WANG X, et al. Synthesis of graphene on a polycrystalline Co film by radio-frequency plasma-enhanced chemical vapour deposition [ J ]. *Journal of Physics D: Applied Physics*, 2010, 43(45) : 455402.
- [ 8 ] VO-VAN C, KIMOUCHE A, RESERBAT-PLANTEY A, et al. Epitaxial graphene prepared by chemical vapor deposition on single crystal thin iridium films on sapphire [ J ]. *Applied Physics Letters*, 2011, 98(18) : 181903.
- [ 9 ] KIM K S, ZHAO Y, JANG H, et al. Large-scale pattern growth of graphene films for stretchable transparent electrodes [ J ]. *Nature*, 2009, 457 : 706-710.
- [ 10 ] KANG B J, MUN J H, HWANG C Y, et al. Monolayer graphene growth on sputtered thin film platinum [ J ]. *Journal of Applied Physics*, 2009, 106(10) : 104309.
- [ 11 ] OZNULUER T, PINCE E, POLAT E O, et al. Synthesis of graphene on gold [ J ]. *Applied Physics Letters*, 2011, 98(18) : 183101.
- [ 12 ] WANG G, ZHANG M, ZHU Y, et al. Direct growth of graphene film on germanium substrate [ J ]. *Scientific Reports*, 2013, 3 : 2465.
- [ 13 ] LEE J H, LEE E K, JOO W J, et al. Wafer-scale growth of single-crystal monolayer graphene on reusable hydrogen-terminated germanium [ J ]. *Science*, 2014, 344(6181) : 286-289.
- [ 14 ] MA L P, REN W C, CHENG H M. Transfer methods of graphene from metal substrates: a review [ J ]. *Small Methods*, 2019, 3(7) : 1900049.
- [ 15 ] WATSON A J, LU W B, GUIMARÃES M H D, et al. Transfer of large-scale two-dimensional semiconductors: challenges and developments [ J ]. *2D Materials*, 2021, 8(3) : 032001.
- [ 16 ] SONG Y Q, ZOU W T, LU Q, et al. Graphene transfer: paving the road for applications of chemical vapor deposition graphene [ J ]. *Small*, 2021, 17(48) : e2007600.
- [ 17 ] AHN Y, KIM H, KIM Y H, et al. Procedure of removing polymer residues and its influences on electronic and structural characteristics of graphene [ J ]. *Applied Physics Letters*, 2013, 102(9) : 091602.
- [ 18 ] ZHUANG B Z, LI S Y, LI S Y, et al. Ways to eliminate PMMA residues on graphene: superclean graphene [ J ]. *Carbon*, 2021, 173 : 609-636.
- [ 19 ] LIU F. Mechanical exfoliation of large area 2D materials from vdW crystals [ J ]. *Progress in Surface Science*, 2021, 96(2) : 100626.
- [ 20 ] LIN Y C, JIN C H, LEE J C, et al. Clean transfer of graphene for isolation and suspension [ J ]. *ACS Nano*, 2011, 5(3) : 2362-2368.
- [ 21 ] LI Z W, REN L W, WANG S Y, et al. Dry exfoliation of large-area 2D monolayer and heterostructure arrays [ J ]. *ACS Nano*, 2021, 15(8) : 13839-13846.
- [ 22 ] LIU L T, KONG L G, LI Q Y, et al. Transferred van der Waals metal electrodes for sub-1-nm MoS<sub>2</sub> vertical transistors [ J ]. *Nature Electronics*, 2021, 4 : 342-347.
- [ 23 ] LIU G Y, TIAN Z A, YANG Z Y, et al. Graphene-assisted metal transfer printing for wafer-scale integration of metal electrodes and two-dimensional materials [ J ]. *Nature Electronics*, 2022, 5 : 275-280.
- [ 24 ] KWON G, CHOI Y H, LEE H, et al. Interaction- and defect-free van der Waals contacts between metals and two-dimensional semiconductors [ J ]. *Nature Electronics*, 2022, 5 : 241-247.
- [ 25 ] KIM H H, YANG J W, JO S B, et al. Substrate-induced solvent intercalation for stable graphene doping [ J ]. *ACS Nano*, 2013, 7(2) : 1155-1162.
- [ 26 ] FERRARI A C, MEYER J C, SCARDACI V, et al. Raman spectrum of graphene and graphene layers [ J ]. *Physical Review Letters*, 2006, 97(18) : 187401.

# 大尺寸单层石墨烯图案的金网转移

李超\*, 姜萌

东华大学 理学院, 上海 201620

**摘要:** 当化学气相沉积 (chemical vapor deposition, CVD) 法制备的石墨烯被应用于各种高性能器件时, 石墨烯的转移和图案化过程通常会降低石墨烯的固有特性。为实现石墨烯图案的高质量和大规模转移, 该研究采用了湿法转移和机械剥离相结合的新方法。这种方法需要制备具有一定孔隙的金网以作为剥离带。接触区 (金箔和石墨烯之间) 能为机械剥离提供足够的黏附力, 以形成均匀的单层石墨烯, 而非接触区 (孔洞和石墨烯之间) 的力相对较弱, 有利于石墨烯图案从基底上释放。石墨烯表面形貌和电学特性表明, 石墨烯表面洁净且均匀, 用该石墨烯制备的场效应晶体管具有高的载流子迁移率和小狄拉克电压。金网转移方法能有效提高石墨烯图案的质量和转移效率, 这为 CVD 法制备石墨烯的应用开辟了更广阔的前景, 同时也为其他二维材料的转移提供了参考。

**关键词:** 石墨烯转移; 石墨烯图案; 金网; 光刻; 晶体管